Acta Cytologica

Fine Needle Aspiration

Acta Cytologica 2026;70:175–184
DOI: 10.1159/000549506

Received: August 12, 2025
Accepted: November 5, 2025
Published online: November 26, 2025

Cytological Features of Metastatic Clear Cell Renal Cell Carcinoma Diagnosed on Cytology: A Single-Center Experience with Literature Review

Isabella Sorice Anna Maria Carillo Maria Salatiello Pasquale Pisapia
Elena Vigliar Giancarlo Troncone Claudio Bellevicine

Department of Public Health, University of Naples "Federico II", Naples, Italy

Keywords
Clear cell renal cell carcinoma · Cytology · Fine-needle aspiration · Metastasis · Immunocytochemistry · Cytomorphology · PAX8 · CD10 · Diagnostic accuracy · Literature review

Abstract

Introduction: Renal cell carcinoma frequently metastasizes to multiple sites, which often poses significant diagnostic challenges, particularly when the primary tumor is unknown or occult. This retrospective study analyzed 43 fine-needle aspiration (FNA) cases of metastatic ccRCC from a single institution to characterize metastatic patterns and evaluate the diagnostic utility of cytology combined with immunocytochemistry. ***Methods:*** We retrospectively reviewed FNA cases diagnosed as metastatic RCC from January 2003 to December 2024. Cytopathological evaluation included cellularity, architectural patterns, cytoplasmic and nuclear features, background elements, and immunocytochemical analysis when available. ***Results:*** Cytology demonstrated excellent diagnostic performance. The majority of cases were reported as malignant (91%), while the remaining 9% were classified as suspicious for malignancy or atypia of undetermined significance. Notably, in 42% of cases, FNA established the initial diagnosis of RCC, highlighting its value in detecting occult primary tumors. Diagnostic accuracy relied on cytomorphologic evaluation, complemented by immunocytochemical profiling, which was performed on cell blocks in 60.4% of cases. ***Conclusion:*** Key markers such as PAX8, CD10, and RCCma were critical in confirming renal origin and differentiating ccRCC from morphologically similar neoplasms in each organ. FNA cytology, corroborated by focused immunocytochemistry, plays a key role in diagnosing metastatic ccRCC, particularly when the presentation is uncommon or the primary tumor is hidden. This integrated method supports effective clinical management, avoiding unnecessary surgery in cases that may benefit from systemic therapy.

Introduction

Clear cell renal cell carcinoma (ccRCC) is the most common subtype of renal cancer, with a rising incidence worldwide. This malignancy accounts for approximately 2–3% of all adult solid tumors, occurring more frequently in males than females and peaking between 60 and 70 years of age. Despite advances in diagnostic and therapeutic approaches, ccRCC remains aggressive and highly prone to metastasize to various anatomical sites [1, 2].

karger@karger.com
www.karger.com/acy

Correspondence to:
Giancarlo Troncone, giancarlo.troncone@unina.it

Karger

While RCC most frequently metastasizes to the lungs, bones, liver, and brain, it can spread to virtually any anatomical location, including highly unusual sites. Such presentations may pose significant diagnostic dilemmas, especially when the patient's clinical history does not immediately suggest a renal primary or when the primary tumor remains occult [3]. Since the primary tumor is often clinically silent, ccRCC metastases may be mistaken for primary tumors of the affected organs [4].

Small tissue sampling, including fine-needle aspiration (FNA) cytology, represents a minimally invasive yet extremely useful approach for identifying the primary site of metastasis, particularly when supported by immunocytochemical stains performed on cell block material or molecular testing [5, 6]. Recently, we reported our experience with the diagnosis of lymph node metastases by FNA, where 6 out of 982 metastases sampled (0.6%) were from ccRCC, including 3 patients with an unknown primary (the naïve group) [7]. However, because ccRCC often metastasizes to unusual extranodal sites [8], we extended our review of this case series, focusing on the role of FNA in the diagnosis of metastatic ccRCC. Specifically, we analyzed the original cytological diagnoses, microscopic findings, and results of ancillary stains, when available.

Materials and Methods

We searched the electronic archive of the University of Naples "Federico II" from January 2003 to December 2024 for FNAs performed on suspected metastatic sites, selecting diagnostic reports that included terms related to ccRCC (e.g., "clear cell carcinoma," "renal cell carcinoma," "renal carcinoma"). Demographic data, including patient sex, age at diagnosis, clinical history, and anatomical site of FNA, were recorded for each case.

At our institution, all FNAs of superficial organs are performed under ultrasound guidance by experienced cytopathologists using 23-gauge needles [9]. The first pass is typically used to prepare a direct smear, which is air-dried and stained with Diff-Quik (Bio-Optica S.p.A) for rapid on-site evaluation, allowing assessment of specimen adequacy and triage. Additional smears are either air-dried and Diff-Quik stained or alcohol-fixed and stained with Papanicolaou. In selected cases, additional material is collected for cell block preparation. FNAs of deep-seated organs are performed by interventional radiologists (e.g., CT-guided lung FNA) or endoscopists (e.g., EUS-guided pancreatic FNA); in these cases, cytopathologists handle the aspirated material as described above.

Cytological reports for FNAs of organs for which a standardized reporting system was not available at the time of the original diagnosis (e.g., Bethesda System for thyroid) were classified using non-standardized categories such as *malignant*, *suspicious*, or *atypical*. For each case, cytological slides were reviewed together with the original reports, and detailed features – including background, cellularity, architectural arrangement, and cytoplasmic and nuclear characteristics – were recorded. When a cell block was available, information on the immunocytochemical profile was also collected. For a small number of older cases, dating back up to 20 years, the original slides could not be retrieved, and only the information from the original cytology reports was used.

When a cell block was available, information on the immunocytochemical profile was also collected. No statistical analysis was performed, as the study aimed to provide a descriptive assessment of cytomorphological patterns and immunocytochemical profiles in a series of metastatic ccRCC cases.

Results

During the 20-year study period, a total of 52 metastatic ccRCC cases were diagnosed at our institution, including 43 cytological cases (which constitute the focus of the present study) and 9 histological cases involving the adrenal gland (n = 1), lung (n = 1), brain (n = 3), upper lip (n = 1), scalp (n = 1), upper labial fornix (n = 1), and femur (n = 1). Notably, none of the histological cases had a prior cytological evaluation to confirm the diagnosis.

The cytological cohort showed a male predominance, with 32 males (74.4%) and 11 females (25.6%), resulting in a male-to-female ratio of 2.9:1. Patient age at diagnosis ranged from 43 to 87 years, with a mean of 64 years.

A history of a previously known primary renal tumor was available in 25 cases (58.1%). Among these, 13 cases (30.2%) had prior histological confirmation of ccRCC within the institutional archives. In the remaining 18 cases (41.9%), the diagnosis of ccRCC was initially established by FNA, without prior knowledge of a renal primary.

Laterality information was available for 32 out of 43 cases and is reported below wherever possible. The most frequently involved anatomical sites were lymph nodes (n = 12; 27.9%), distributed as follows: supraclavicular (right n = 2, left n = 2), inguinal (right n = 2, left n = 1),

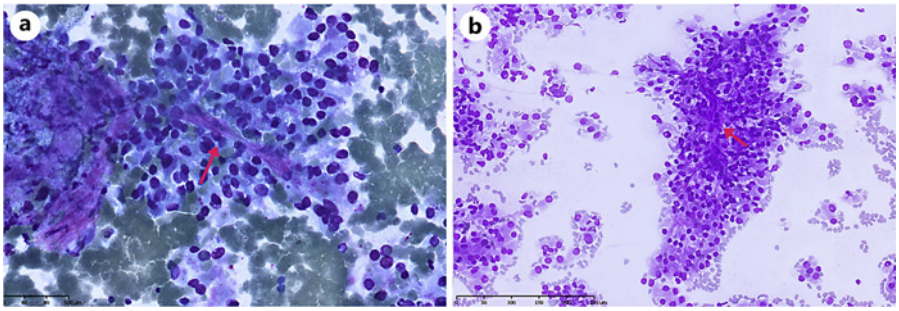

Fig. 1. a, **b** Neovascularization in ccRCC. Newly formed capillaries (red arrows) traverse clusters of neoplastic cells, highlighting the prominent vascularity typical of this tumor (MGG, ×200).

laterocervical (right $n = 2$, left $n = 1$), axillary (left $n = 1$), and peribronchial ($n = 1$). Other common sites included bone ($n = 7$; 16.3%) with lesions in the D12 vertebral body and the fifth right rib; lung ($n = 6$; 14.0%) with nodules in the left lower lobe, right lower lobe, and apical segment of the right upper lobe; thyroid ($n = 5$; 11.6%) with nodules in the isthmus, left lobe, and right lobe; salivary glands ($n = 4$; 9.3%) involving the left and right parotid and left submandibular regions; and soft tissues ($n = 4$; 9.3%) located in the left hypochondrium, right shoulder, scalp, and forehead. Less frequent sites were the pancreas ($n = 2$; 4.7%) and retroperitoneal region ($n = 1$; 2.3%). Additional lesions included superficial nodules on the forehead and right mandibular region, and a lesion at the S3 level of the retrosacral region.

Of the 43 cases, the majority were diagnosed as malignant (39 cases, 91%). Among the remaining 4 cases (9%), three were classified as suspicious for malignancy, involving the thyroid, lung, and pancreas, while one case was reported as atypia of undetermined significance in the salivary gland.

A detailed cytological description was ensured for each case through direct review of the cytological slides. The most frequently reported background was hemorrhagic (23 cases; 53.5%). Neovascularization was observed in 5 cases (11.6%), characterized by newly formed capillaries traversing clusters of neoplastic cells – a striking feature reflecting the highly vascular nature of ccRCC and serving as a valuable diagnostic clue (Fig. 1). Less common background elements included site-specific components such as lymphoid cells (7 cases; 16.3%), alveolar macrophages, thyroid follicular cells, hepatocyte-like cells, osteoclasts, and necrosis.

Cellularity was reported as hypercellular in 8 cases (18.6%), moderately cellular in 11 cases (25.6%), and hypocellular in 4 cases (9.3%). Architectural patterns included cohesive cell groups in 8 cases (18.6%), single-cell dispersal in 4 cases (9.3%), and a combination of both in 9 cases (20.9%).

The most commonly observed cytomorphological features (38/43 cases, 88%) included abundant, clear to finely granular cytoplasm, and atypical round-to-oval nuclei with prominent nucleoli, defined as nucleoli clearly visible at low-to-medium magnification, well delimited, and occupying ≥20% of the nuclear diameter in medium-to-large cells, particularly when atypical (18/43 cases, 42%) [10]. Two cases showed oncocytic differentiation; however, these cells were admixed with cells exhibiting clear cytoplasm, consistent with ccRCC origin. In cases where it could be assessed, cytoplasmic vacuolization was evaluated according to predefined criteria, defined as cytoplasm containing at least 50% clear, well-defined vacuoles with sharp borders [11]. Two cases metastatic to the liver and soft tissue, respectively, were diagnosed thanks to immunocytochemical analysis due to their high-grade features and lack of morphological differentiation (Table 1).

Cytopathological diagnoses were standardized into reproducible categories: ccRCC, oncocytic ccRCC, moderately differentiated ccRCC, poorly differentiated/anaplastic RCC, and generic epithelial malignancy with renal primitivity (Table 1), the latter showing clear cell features upon cytological reevaluation. Immunocytochemical analysis was performed in most cases on cell block sections (26/43; 60.4%). The most frequently employed renal markers included PAX8 (10/11 positive, 91%) and renal cell carcinoma marker (7/9 positive, 77.8%). CD10, commonly expressed in ccRCC due to proximal tubular differentiation, was positive in all cases tested (20/20; 100%), though its expression reflects phenotypic features of clear cells rather than a definitive tissue-specific marker [12]. Although carbonic anhydrase IX [13] is recognized as a sensitive marker for ccRCC, it was unavailable in our laboratory during the study period. A complete summary of immunocytochemical results is provided in Table 2.

Table 1. Demographic and tumor-related data of the study cohort

N	Year	Clinical history	ICC	Diagnosis	Relevant cytology features	Location
1	2003	RCC (2000)	N.P.[a]	Malignant; ccRCC	Medium epithelial cells; vacuolated cytoplasm	D12 vertebral body
2	2003		N.P.	Malignant; moderately differentiated RCC	Medium epithelial cells; vacuolated cytoplasm	Right scapular glenoid
3	2004		PanCK	Malignant; oncocytic ccRCC	Polygonal cells; microvacuolated/ granular cytoplasm; oncocytic cells	Left cervical lymph node
4	2005		PanCk, S100	Malignant; oncocytic ccRCC	Oncocytic cells; *lymphocytes*	Left supraclavicular lymph node
5	2005		PanCK, HMB-45	Malignant; moderately differentiated RCC	Granular cytoplasm	Right lung
6	2006	RCC (2001)	N.P.	Malignant; moderately differentiated RCC	Clear cytoplasm; epithelial cells; *alveolar macrophages*	Right lung
7	2006		N.P.	Malignant; ccRCC	Clear and vacuolated cytoplasm; transgressing vessels	Bone
8	2007		N.P.	Malignant; ccRCC	Granular cytoplasm	Left hypochondrium
9	2007		N.P.	Malignant; poorly differentiated RCC	Vacuolated cytoplasm	Right and left inguinal regions, lymph nodes
10	2007	RCC (2006)	Vimentin	Malignant; ccRCC	Vacuolated cytoplasm	Lung
11	2007		N.P.	Malignant; ccRCC	Vacuolated cytoplasm	Lung
12	2008	RCC	N.P.	Malignant; ccRCC	Clear and vacuolated cytoplasm; *hepatocytes*	Liver
13	2008		N.P.	Malignant; ccRCC	Clear and vacuolated cytoplasm; *osteoclasts*	Bone
14	2009		N.P.	Malignant; ccRCC	Vacuolated cytoplasm; multinucleated cells	Retroperitoneal region
15	2010		CD10, CK20	Malignant; ccRCC	Vacuolated cytoplasm	Supraclavicular lymph node
16	2010		N.P.	Malignant; ccRCC	*Mature lymphocytes*	Left laterocervical lymph node
17	2011	RCC	CD10	Malignant; ccRCC	*Mature lymphocytes*	Left inguinal lymph nodes
18	2011		CD10, CK7, PanCK, TTF-1	Malignant; moderately differentiated RCC	Vacuolated cytoplasm; necrotic background; transgressing vessels	Right laterocervical lymph node
19	2012	RCC (2012)	N.P.	Malignant; ccRCC	Vacuolated cytoplasm	Left supraclavicular lymph node
20	2013		CD10, CK7, PanCK, TTF-1	Malignant; ccRCC	Vacuolated cytoplasm; multinucleated cells; *mature lymphocytes*	Left lumbar-aortic lymph node
21	2014	RCC	PAX8	Malignant; ccRCC	Granular cytoplasm	Peribronchial lymph node
22	2014	RCC (2000)	PAX8, CD10, RCCma, TTF-1	Malignant; ccRCC	Vacuolated cytoplasm; *thyrocytes*	Thyroid, right lobe

Table 1 (continued)

N	Year	Clinical history	ICC	Diagnosis	Relevant cytology features	Location
23	2014	RCC	CD10, TTF-1	Malignant; ccRCC	Clear and vacuolated cytoplasm; transgressing vessels	Thyroid, right lobe
24	2015		N.P.	Malignant; ccRCC	Vacuolated cytoplasm	Right 5th rib
25	2015	RCC (2015)	CD10, PAX8	Malignant ccRCC	Microvacuolated/eosinophilic cytoplasm; *mature lymphocytes*	Right supraclavicular region lymph node
26	2016		PanCK, CD10, PAX8, TTF-1, S100	Malignant; poorly differentiated/ anaplastic RCC	Bi/multinucleated cells; elongated cytoplasm	Right shoulder
27	2017	U.N.[b] (2017)	PAX8, CD10, RCCma, HepPar	Malignant; poorly differentiated RCC	Large cells; marked nuclear atypia	Liver
28	2017	RCC (2011)	PAX8	Malignant; ccRCC	Clear and vacuolated cytoplasm	Soft tissue
29	2017		N.P.	Malignant; ccRCC	Clear granular cytoplasm; atypical nuclei; prominent nucleoli; transgressing vessels	Left lung, lower lobe
30	2017	RCC (2011)	N.P.	Malignant; ccRCC	Vacuolated cytoplasm	Left radius
31	2018	RCC (2015)	CD10, RCCma	Malignant; ccRCC	Clear and vacuolated cytoplasm	Pancreas
32	2019	RCC (2015)	N.P.	Malignant; ccRCC	Clear and vacuolated cytoplasm	Thyroid, isthmus
33	2019	RCC	CD10, RCCma	SFM; ccRCC	Vacuolated cytoplasm; prominent nucleoli	Forehead
34	2019	RCC	CD10, RCCma	Malignant; ccRCC	Clear cytoplasm; stromal fragments	Left submandibular gland
35	2019	RCC (2019)	CD10, RCCma, PAX8	Atypical; ccRCC	Clear cytoplasm	Left parotid
36	2019	RCC (2011)	CD10, RCCma, PAX8	Malignant; ccRCC	Atypical epithelial cells	Pancreatic body
37	2020		CD10, PAX8, PSA, CK7	SFM; ccRCC	Clear cytoplasm; atypical nuclei	Retrosacral lesion at S3 level
38	2021		PAX8, CD10, RCCma, GATA3, WT1	Malignant; generic epithelial malignancy with renal primitivity	Vacuolated cytoplasm; *neutrophils*	Right inguinal lymph node
39	2021	RCC (2019)	CD10, RCCma, TTF-1	Malignant; ccRCC	Vacuolated cytoplasm	Thyroid, right lobe
40	2024	RCC (2018)	N.P.	Malignant; ccRCC	Vacuolated cytoplasm	Lung, right upper lobe
41	2024	RCC (2024)	CD10	SFM; ccRCC	Clear cytoplasm; atypical nuclei; *mature lymphocytes*	Right mandibular region
42	2024	RCC (2021)	CD10	Malignant; ccRCC	Vacuolated cytoplasm; transgressing vessels	Thyroid, right lobe
43	2024	RCC	CD10, PAX8	Malignant; ccRCC	Microvacuolated cytoplasm	Right parotid

Italicized elements indicate background cellular components typical of the site. SFM, suspicious for malignancy; RCCma, renal cell carcinoma marker. [a]N.P. as non-performed. [b]U.N. as undifferentiated neoplasm.

Table 2. Immunocytochemical results for key markers in metastatic renal cell carcinoma cases

Marker	Positive cases/total tested	Staining pattern
PAX8	10/11 (91%)	Nuclear
Pancytokeratin	8/8 (100%)	Cytoplasmic
CD10	20/20 (100%)	Membranous
RCCma	7/9 (77.8%)	Cytoplasmic/membranous

RCCma, renal cell carcinoma marker.

Discussion

The metastatic spread of ccRCC significantly influences patient prognosis and treatment planning. Accurate detection of these metastases, particularly in varied and anatomically challenging locations, is essential for proper staging and effective therapeutic strategies [14]. In this context, FNA can provide valuable diagnostic information and help refine the differential diagnosis.

While initial diagnostic clues may be evident from standard cytomorphological evaluation, a definitive diagnosis often requires a comprehensive immunocytochemical workup. This is particularly important given that the "clear cell" appearance characteristic of ccRCC is shared by a wide range of other neoplasms. The anatomical distribution of metastases in our cohort highlights the often-unpredictable metastatic tropism of ccRCC, emphasizing the need for clinicians and pathologists to consider a renal primary in the differential diagnosis of clear cell lesions, regardless of their location, especially when the primary tumor is unknown [1, 2, 15].

In this context, it is helpful to consider ccRCC within the broader spectrum of renal cell carcinomas. ccRCC is the most common subtype, representing about 70–75% of cases. Papillary RCC accounts for 10–15% and is often composed of small to medium cells arranged in papillary or tubulopapillary structures, sometimes with foamy macrophages. Chromophobe RCC is rare and shows large polygonal cells with pale or eosinophilic cytoplasm, distinct cell borders, and perinuclear halos. In cytologic preparations, ccRCC typically appears as loosely cohesive clusters or single large epithelioid cells with abundant clear cytoplasm, well-defined borders, and prominent nucleoli. Papillary RCC may show papillary fragments or more cohesive clusters, while chromophobe RCC often exhibits solid sheets with prominent cell membranes and perinuclear clearing [15]. Recognizing these cytologic patterns can help guide the differential diagnosis and inform the selection of immunocytochemical markers, particularly in metastatic lesions where the primary site is unknown.

A notable finding of our study was that in 42% of cases (18/43), the diagnosis of ccRCC was first established through FNA cytology of a metastatic site, before identification of a primary renal tumor. This highlights FNA's essential role as a minimally invasive, cost-effective tool for early detection of occult malignancies, guiding subsequent diagnostic workup and timely clinical management. In the remaining cases where the primary tumor was known, FNA was valuable for confirming metastatic spread and informing therapeutic decisions. Additionally, the use of cell blocks and immunocytochemistry in over 60% of FNAs enhanced diagnostic precision, particularly for subtyping complex clear cell lesions when morphology alone was insufficient [12].

In most metastatic ccRCC with previously unknown renal primary, the diagnosis was initially suspected on microscopic observation of large epithelioid tumor cells with abundant clear cytoplasm, distinct cell borders, and prominent nucleoli (Fig. 2). In a minority of cases (5/43; 11.6%), the presence of endothelial cells forming vascular structures provided an additional strong clue for the diagnosis of ccRCC (Fig. 1). However, the "clear cell" morphology is not exclusive to ccRCC, necessitating immunocytochemical confirmation. Markers such as PAX8, CD10, and RCC antigen are crucial for distinguishing ccRCC from cytological mimics.

Our analysis of 43 cases collected over a 20-year period demonstrates a clear evolution in ICC diagnostic practices. During the first period (2003–2010), most cases lacked ICC characterization (64.7%), while those assessed with 2–3 markers accounted for 35.3%. In contrast, during the second period (2011–2024), the proportion of cases without ICC markedly decreased to 23.1%, whereas cases characterized with 2–3 renal-specific markers increased to 50%, and those evaluated with extended panels (≥6 markers) rose to 26.9%. This trend reflects a transition from sporadic and limited ICC

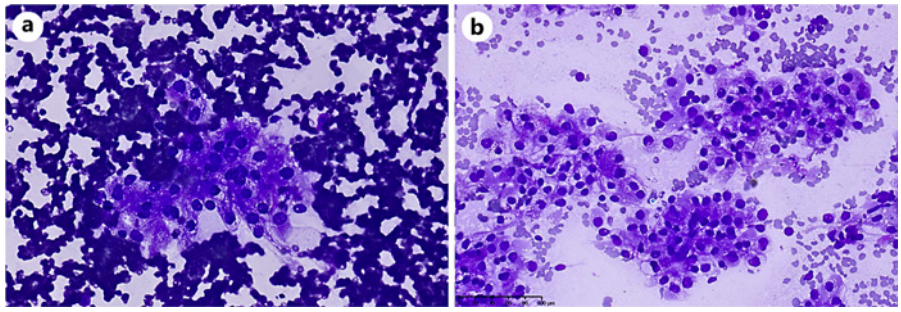

Fig. 2. a, **b** Cytological counterpart of Figure 1. Neoplastic cells show abundant clear to finely granular cytoplasm and atypical round-to-oval nuclei, consistent with the characteristic morphology of ccRCC in cytological specimens. **a** MGG, ×200. **b** MGG, ×400.

Table 3. Differential diagnosis strategies based on metastatic site

Site	Rule out	ICC markers
Lung	Primary lung adenocarcinoma	TTF-1+, napsin A+, CK7+, PAX8–
Lymph node	Clear cell melanoma	S100+, HMB45+, MART-1+, SOX10+, PRAME+
	Gynecologic clear cell carcinoma	HNF1β+, napsin A+, CK7+, ER–, PAX8+/–
	Adrenocortical carcinoma	SF1+, MART-1+, inhibin+, calretinin+, synaptophysin+
Thyroid	Follicular/papillary carcinoma (clear cell variant)	TTF-1+, thyroglobulin+, PAX8+
	Medullary thyroid carcinoma (clear cell variant)	Calcitonin+, CEA+, RET mutation+
Salivary gland	Acinic cell carcinoma	DOG1+, SOX10+, CK7+, PAS+ (zymogen granules), NR4A3+
	Hyalinizing clear cell carcinoma	EWSR1 rearrangement+, CK7+, p63+
	Mucoepidermoid carcinoma	CK7+, p63+, MUC5AC+, MAML2 rearrangement+
Bone	Metastatic prostate adenocarcinoma	PSA+, PSAP+, NKX3.1+
	Metastatic breast carcinoma	ER+, PR+, GATA3+, mammaglobin+
	Metastatic lung adenocarcinoma	TTF-1+, napsin A+, CK7+
	Clear cell chondrosarcoma	S100+ (variable), SOX9+
Soft tissue	Clear cell sarcoma	SOX10+, HMB45+, MART-1+, EWSR1 rearrangement+
Female genital tract	Clear cell carcinoma	HNF1β+, napsin A+, CK7+, ER–

analyses – typically restricted to cytokeratin and vimentin – to a more systematic and targeted application of renal-specific panels. Notably, in the later period, the absence of ICC data was exclusively attributable to unavailable clinical information rather than technical limitations.

Overall, over 2 decades, there has been a clear progression from a predominance of non-characterized cases (39.5%) to a majority of well-characterized ones (44.2% with 2–3 markers and 16.3% with ≥6 markers), underscoring a substantial improvement in diagnostic accuracy and the progressive adoption of comprehensive immunocytochemical approaches. The main differential diagnoses and relevant immunocytochemical markers are summarized in Table 3. In our series, lymph nodes were the most frequent metastatic site (27.9%). Cytological assessment of clear cell metastases is challenging because ccRCC, gynecologic clear cell carcinomas, and other neoplasms share overlapping morphologic features such as clear cytoplasm, prominent nucleoli, and nested or tubulocystic patterns, often lacking site-specific clues [9]. Ovarian high-grade serous carcinoma, metastatic melanoma, and adrenocortical carcinoma may mimic ccRCC, emphasizing the need for careful evaluation [16–24].

Bone was the second most common metastatic site (16.3%). Cytologic diagnosis of clear cell tumors in bone is complicated by limited architectural context. Metastatic ccRCC typically appears as loosely cohesive clusters or single cells with abundant clear cytoplasm,

but similar features may be seen in metastases from prostate, breast, or lung carcinomas [25, 26]. Rare primary bone tumors, such as clear cell chondrosarcoma, can also mimic ccRCC, requiring clinical correlation and immunocytochemical confirmation [27–29].

Lung metastases represented the third most frequent extranodal site (14.0%) and are among the most challenging scenarios. ccRCC may closely resemble primary lung adenocarcinomas with clear cytoplasm, particularly in small biopsies or cytology specimens. The so-called clear cell adenocarcinoma of the lung is no longer recognized as a distinct subtype [30, 31]. The rare primary lung hyalinizing clear cell carcinoma should only be considered after metastatic disease has been excluded [32–34].

Although less common, thyroid metastases accounted for 11.6% of cases, all in patients with a known primary ccRCC. Distinguishing metastatic ccRCC from primary clear cell thyroid tumors can be difficult due to overlapping morphology [35–37]. Similarly, metastases to the salivary glands were rare (9.3%), and ccRCC may mimic primary salivary tumors with clear cell features, including lesions in the SUMP category, which carry increased malignancy risk [38–42].

In summary, the widespread occurrence of clear cell morphology across diverse tumor types underscores the need for a carefully selected immunocytochemical panel, tailored to the clinical and anatomic context. Integrating morphologic features with immunocytochemical markers enables accurate identification of metastatic ccRCC and effective distinction from its histologic mimics, ultimately guiding appropriate clinical management. One of the limits of this study is the lack of availability at our center of carbonic anhydrase IX, one of the most useful markers to narrow down the ccRCC diagnosis. However, other markers included in our immunocytochemical workup on cell blocks such as CD10, PAX8, and renal cell carcinoma marker used in combination were sufficient in most cases.

Conclusion

Our institutional experience highlights the heterogeneity of metastatic ccRCC in both patient demographics and anatomical distribution. FNA has proven to be an effective first-line modality for the cytopathological diagnosis of occult primary renal tumors. Accurate identification of ccRCC metastases depends on the integration of cytomorphologic assessment with a targeted immunohistochemical panel, guided by a comprehensive understanding of marker expression profiles. This diagnostic framework is essential for informing appropriate clinical management and optimizing patient outcomes in the context of metastatic ccRCC.

Statement of Ethics

Institutional Review Board approval was waived by the Comitato Etico Università Federico II – A.O.U. Federico II, Naples, Italy, as this study was retrospective and did not require any deviation from the standard of care. Written informed consent was obtained from patients or their legal guardians to participate in studies involving the collection of clinical-pathological data. Written informed consent was also obtained for the publication of the clinical details and any accompanying images, in accordance with the Declaration of Helsinki (https://www.wma.net/policies-post/wma-declaration-of-helsinki-ethical-principles-for-medical-research-involving-human-subjects/). Moreover, consent was obtained in compliance with the general authorization for processing personal data for scientific research purposes from "The Italian Data Protection Authority" (http://www.garanteprivacy.it/web/guest/home/docweb/-/docwebdisplay/export/2485392). All information regarding human material was managed using anonymous numerical codes, and all samples were handled in compliance with the ethical principles.

Conflict of Interest Statement

The authors have no conflicts of interest to declare.

Funding Sources

This research did not receive any specific grant from funding agencies in the public, commercial, or not-for-profit sectors.

Author Contributions

Conceptualization: Isabella Sorice, Giancarlo Troncone, and Claudio Bellevicine. Methodology, data curation, and writing – review and editing: Isabella Sorice, Anna Maria Carillo, Giancarlo Troncone, and Claudio Bellevicine. Investigation and resources: Isabella Sorice, Anna Maria Carillo, Maria Salatiello, Pasquale Pisapia, Elena Vigliar, Giancarlo Troncone, and Claudio Bellevicine. Writing – original draft preparation: Isabella Sorice, Anna Maria Carillo, and Claudio Bellevicine. Visualization: Isabella Sorice. Supervision: Anna Maria Carillo, Giancarlo Troncone, and Claudio Bellevicine.

Data Availability Statement

The data that support the findings of this study are available on request from the corresponding author. The data are not publicly available due to privacy or ethical restrictions.

References

1 Bahadoram S, Davoodi M, Hassanzadeh S, Bahadoram M, Barahman M, Mafakher L. Renal cell carcinoma: an overview of the epidemiology, diagnosis, and treatment. G Ital Nefrol. 2022;39(3):2022-vol3.

2 Capitanio U, Bensalah K, Bex A, Boorjian SA, Bray F, Coleman J, et al. Epidemiology of renal cell carcinoma. Eur Urol. 2019;75(1):74–84. https://doi.org/10.1016/j.eururo.2018.08.036

3 Morita Y, Kashima K, Suzuki M, Kinosada H, Teramoto A, Matsumiya Y, et al. Differential diagnosis between oral metastasis of renal cell carcinoma and salivary gland cancer. Diagnostics. 2021;11(3):506. https://doi.org/10.3390/diagnostics11030506

4 Tabatabai ZL, Staerkel GA. Distinguishing primary and metastatic conventional renal cell carcinoma from other malignant neoplasms in fine-needle aspiration biopsy specimens. Arch Pathol Lab Med. 2005;129(8):1017–21. https://doi.org/10.5858/2005-129-1017-DPAMCR

5 Carillo AM, De Luca C, Nacchio M, Salatiello M, Pisapia P, Damiano V, et al. A challenging case of enteric-type lung adenocarcinoma metastatic to the thyroid harboring RET-fusion diagnosed on fine-needle aspiration. Virchows Arch. 2025;486(1):1–5. https://doi.org/10.1007/s00428-025-04093-7

6 Elsheikh TM, Silverman JF. Fine needle aspiration and core needle biopsy of metastatic malignancy of unknown primary site. Mod Pathol. 2019;32(Suppl 1):58–70. https://doi.org/10.1038/s41379-018-0149-9

7 Acanfora G, Iaccarino A, Dello Iacovo F, Pisapia P, De Luca C, Giordano C, et al. A roadmap for a comprehensive diagnostic approach to fine needle cytology of lymph node metastases. Cytopathology. 2022;33(6):668–77. https://doi.org/10.1111/cyt.13172

8 Sorice I, Carillo AM, Salatiello M, De Luca C, Di Crescenzo RM, Damiano V, et al. Clear cell neoplasm in salivary gland FNA? Maybe it's from kidney. Cytopathology. 2025;36(4):426–9. https://doi.org/10.1111/cyt.13506

9 Vigliar E, Carillo AM, Nacchio M, Cozzolino D, Acanfora G, Salatiello M, et al. The evolving role of interventional cytopathology from thyroid FNA to NGS: lessons learned at Federico II university of Naples. Cytopathology. 2025;36(4):307–17. https://doi.org/10.1111/cyt.13415

10 Jhala N, Siegal GP, Jhala D. Large, clear cytoplasmic vacuolation: an underrecognized cytologic clue to distinguish solid pseudopapillary neoplasms of the pancreas from pancreatic endocrine neoplasms on fine-needle aspiration. Cancer. 2008;114(4):249–54. https://doi.org/10.1002/cncr.23595

11 Li Y, Jia S, Yao Y, Zhou Y, Li S, Li J, et al. The novel role of cytomorphology from ultrasound-guided fine needle aspiration cytology in evaluating the status of prognostic factors including estrogen receptor, progesterone receptor and HER2 in breast cancer. Anal Cell Pathol. 2022;2022:6302751. https://doi.org/10.1155/2022/6302751

12 Reuter VE, Argani P, Zhou M, Delahunt B. Best practices recommendations in the application of immunohistochemistry in kidney tumors: report from the International Society of Urologic pathology consensus conference. Am J Surg Pathol. 2014;38(8):e35–49. https://doi.org/10.1097/PAS.0000000000000258

13 Ordoñez NG. Value of PAX8 immunostaining in tumor diagnosis: a review and update. Adv Anat Pathol. 2012;19(3):140–51. https://doi.org/10.1097/PAP.0b013e318253465d

14 Bi K, He MX, Bakouny Z, Kanodia A, Napolitano S, Wu J, et al. Tumor and immune reprogramming during immunotherapy in advanced renal cell carcinoma. Cancer Cell. 2021;39(5):649–61.e5. https://doi.org/10.1016/j.ccell.2021.02.015

15 Dudani S, De Velasco G, Wells JC, Gan CL, Donskov F, Porta C, et al. Evaluation of clear cell, papillary, and chromophobe renal cell carcinoma metastasis sites and association with survival. JAMA Netw Open. 2021;4(1):e2021869. https://doi.org/10.1001/jamanetworkopen.2020.21869

16 Xu Y, Liu B, Zhang X, Chen L. Cytological features of ovarian or tubal high-grade serous carcinoma: a retrospective study of 12 cases with abnormal cervical liquid-based smear. Diagn Cytopathol. 2021;49(11):1207–12. https://doi.org/10.1002/dc.24871

17 Fadare O, Desouki MM, Gwin K, Hanley KZ, Jarboe EA, Liang SX, et al. Clear cell renal cell carcinoma metastatic to the gynecologic tract: a clinicopathologic analysis of 17 cases. Int J Gynecol Pathol. 2018;37(6):525–35. https://doi.org/10.1097/PGP.0000000000000466

18 Kaspar HG, Crum CP. The utility of immunohistochemistry in the differential diagnosis of gynecologic disorders. Arch Pathol Lab Med. 2015;139(1):39–54. https://doi.org/10.5858/arpa.2014-0057-RA

19 Katcher AH, Greenman MP, Roychoudhury S, Goldberg GL. Utilization of immunohistochemistry in gynecologic tumors: an expert review. Gynecol Oncol Rep. 2024;56:101550. https://doi.org/10.1016/j.gore.2024.101550

20 Murali R, Davidson B, Fadare O, Carlson JA, Crum CP, Gilks CB, et al. High-grade endometrial carcinomas: morphologic and immunohistochemical features, diagnostic challenges and recommendations. Int J Gynecol Pathol. 2019;38 Suppl 1(Iss 1 Suppl 1):S40–63. https://doi.org/10.1097/PGP.0000000000000491

21 Cazzato G, Cascardi E, Colagrande A, Cimmino A, Ingravallo G, Lospalluti L, et al. Balloon cell melanoma: presentation of four cases with a comprehensive review of the literature. Dermatopathology. 2022;9(2):100–10. https://doi.org/10.3390/dermatopathology9020013

22 Spera JA, Pollack HM, Banner MP, Brennan RE, Wein AJ. Metastatic malignant melanoma mimicking renal cell carcinoma. J Urol. 1984;131(4):740–2. https://doi.org/10.1016/s0022-5347(17)50605-9

23 Kanjilal B, Ghosh M, Mitra A, Kar S, Bisht J, Das RN, et al. Cytological diagnosis of adrenocortical carcinoma: a report of 2 cases in children. Diagn Cytopathol. 2018;46(12):1064–7. https://doi.org/10.1002/dc.24056

24 Sangoi AR, Fujiwara M, West RB, Montgomery KD, Bonventre JV, Higgins JP, et al. Immunohistochemical distinction of primary adrenal cortical lesions from metastatic clear cell renal cell carcinoma: a study of 248 cases. Am J Surg Pathol. 2011;35(5):678–86. https://doi.org/10.1097/PAS.0b013e3182152629

25 WHO Classification of Tumours Editorial Board. Soft tissue and bone tumours. 5th ed. Lyon: International Agency for Research on Cancer (IARC); 2020.

26 Huang Z, Du Y, Zhang X, Liu H, Liu S, Xu T. Clear cell renal cell carcinoma bone metastasis: what should be considered in prognostic evaluation. Eur J Surg Oncol. 2019;45(7):1246–52. https://doi.org/10.1016/j.ejso.2019.01.221

27 Zhang Y, Alagic Z, Tani E, Skorpil M, Tsagkozis P, Haglund F. Clear-cell chondrosarcomas: fine-needle aspiration cytology, radiological findings, and patient demographics of a rare entity. Diagn Cytopathol. 2021;49(1):46–53. https://doi.org/10.1002/dc.24582

28 Masui F, Ushigome S, Fujii K. Clear cell chondrosarcoma: a pathological and immunohistochemical study. Histopathology. 1999;34(5):447–52. https://doi.org/10.1046/j.1365-2559.1999.00656.x

29 Matsuura S, Ishii T, Endo M, Takahashi Y, Setsu N, Yamamoto H, et al. Epithelial and cartilaginous differentiation in clear cell chondrosarcoma. Hum Pathol. 2013;44(2):237–43. https://doi.org/10.1016/j.humpath.2012.05.012

30 Komiya T, Guddati AK, Nakanishi Y. Clear cell adenocarcinoma of the lung: a SEER analysis. Transl Lung Cancer Res. 2019;8(2):187–91. https://doi.org/10.21037/tlcr.2018.10.13

31 WHO classification of thoracic tumours. 5th ed. Lyon: International Agency for Research on Cancer (IARC); 2021.

32 Mansur A, Saleem Z, Potter AL, Mathey-Andrews C, Senthil P, Yang CFJ. Primary clear cell adenocarcinoma of the lung: a national analysis. J Thorac Dis. 2023;15(8):4248–61. https://doi.org/10.21037/jtd-23-76

33 Doxtader EE, Shah AA, Zhang Y, Wang H, Dyhdalo KS, Farver C. Primary salivary gland-type tumors of the tracheobronchial tree diagnosed by transbronchial fine needle aspiration: clinical and cytomorphologic features with histopathologic correlation. Diagn Cytopathol. 2019;47(11):1168–76. https://doi.org/10.1002/dc.24285
34 Wang X, Hu S, Lu H. Pulmonary salivary gland tumor–hyalinizing clear cell carcinoma: a literature review. Diagn Pathol. 2024;19(1):37–9. https://doi.org/10.1186/s13000-024-01460-x
35 Chung AY, Tran TB, Brumund KT, Weisman RA, Bouvet M. Metastases to the thyroid: a review of the literature from the last decade. Thyroid. 2012;22(3):258–68. https://doi.org/10.1089/thy.2010.0154
36 Val-Bernal JF, Martino M. Clear cell change in follicular adenoma of the thyroid. A diagnostic challenge. Rom J Morphol Embryol. 2020;61(1):219–26. https://doi.org/10.47162/RJME.61.1.24
37 Heffess CS, Wenig BM, Thompson LD. Metastatic renal cell carcinoma to the thyroid gland: a clinicopathologic study of 36 cases. Cancer. 2002;95(9):1869–78. https://doi.org/10.1002/cncr.10901
38 Gupta S, Alruwaili KHA, Escobedo RLO, Pangarkar M, Chawla JPS, Sunitha S, et al. Renal cell carcinoma metastasizing to salivary glands: systematic review. Natl J Maxillofac Surg. 2024;15(1):3–17. https://doi.org/10.4103/njms.njms_79_23
39 Rocca BJ, Gini A, Calandra C, Ginori A, Crivelli F. Parotid metastasis of renal cell carcinoma, mimicking primary clear cell oncocytoma: report of a case and brief review of the literature. Pathologica. 2017;109(4):384–8.
40 Skálová A, Hyrcza MD, Leivo I. Update from the 5th edition of the world health organization classification of head and neck tumors: Salivary glands. Head Neck Pathol. 2022;16(1):40–53. https://doi.org/10.1007/s12105-022-01420-1
41 Rossi ED, Baloch Z, Barkan G, Foschini MP, Kurtycz D, Pusztaszeri M, et al. Second edition of the milan system for reporting salivary gland cytopathology: refining the role of salivary gland FNA. J Am Soc Cytopathol. 2024;13(1):67–77. https://doi.org/10.1016/j.jasc.2023.08.004
42 Chowsilpa S, An D, Maleki Z. Adenoid cystic carcinoma cytology: salivary gland and nonsalivary gland. Diagn Cytopathol. 2020;48(12):1282–9. https://doi.org/10.1002/dc.24573